MGH–USC Human Connectome Project datasets with ultra-high *b*-value diffusion MRI

Qiuyun Fan [a,1], Thomas Witzel [a,1], Aapo Nummenmaa [a], Koene R.A. Van Dijk [a,b], John D. Van Horn [c],
Michelle K. Drews [a,b], Leah H. Somerville [b], Margaret A. Sheridan [d], Rosario M. Santillana [d], Jenna Snyder [d],
Trey Hedden [a], Emily E. Shaw [a], Marisa O. Hollinshead [a,b], Ville Renvall [a,e], Roberta Zanzonico [a], Boris Keil [a],
Stephen Cauley [a], Jonathan R. Polimeni [a], Dylan Tisdall [a], Randy L. Buckner [a,b], Van J. Wedeen [a],
Lawrence L. Wald [a,f], Arthur W. Toga [c], Bruce R. Rosen [a,f,*]

[a] Athinoula A. Martinos Center for Biomedical Imaging, Department of Radiology, Harvard Medical School, Massachusetts General Hospital, 149 13th Street, Charlestown 02129, MA, USA
[b] Harvard University Department of Psychology, Center for Brain Science, Cambridge, MA, USA
[c] Laboratory of Neuro Imaging, Institute for Neuroimaging and Informatics, Department of Neurology, Keck School of Medicine, University of Southern California, Los Angeles, CA, USA
[d] Division of Developmental Medicine, Boston Children's Hospital, Harvard Medical School, Boston, MA, USA
[e] Department of Neuroscience and Biomedical Engineering, Aalto University School of Science, Espoo, Finland
[f] Harvard — MIT Division of Health Sciences and Technology, Massachusetts Institute of Technology, Cambridge, MA, USA

ARTICLE INFO

ABSTRACT

The MGH–USC CONNECTOM MRI scanner housed at the Massachusetts General Hospital (MGH) is a major hardware innovation of the Human Connectome Project (HCP). The 3T CONNECTOM scanner is capable of producing a magnetic field gradient of up to 300 mT/m strength for *in vivo* human brain imaging, which greatly shortens the time spent on diffusion encoding, and decreases the signal loss due to T2 decay. To demonstrate the capability of the novel gradient system, data of healthy adult participants were acquired for this MGH–USC Adult Diffusion Dataset ($N = 35$), minimally preprocessed, and shared through the Laboratory of Neuro Imaging Image Data Archive (LONI IDA) and the WU–Minn Connectome Database (ConnectomeDB). Another purpose of sharing the data is to facilitate methodological studies of diffusion MRI (dMRI) analyses utilizing high diffusion contrast, which perhaps is not easily feasible with standard MR gradient system. In addition, acquisition of the MGH–Harvard–USC Lifespan Dataset is currently underway to include 120 healthy participants ranging from 8 to 90 years old, which will also be shared through LONI IDA and ConnectomeDB. Here we describe the efforts of the MGH–USC HCP consortium in acquiring and sharing the ultra-high *b*-value diffusion MRI data and provide a report on data preprocessing and access. We conclude with a demonstration of the example data, along with results of standard diffusion analyses, including *q*-ball Orientation Distribution Function (ODF) reconstruction and tractography.

© 2015 Elsevier Inc. All rights reserved.

Introduction

The NIH Blueprint for Neuroscience Research has funded the MGH–USC consortium of the Human Connectome Project (HCP) to build a one of a kind CONNECTOM scanner. It is based on a Siemens Skyra 3T platform (Siemens Healthcare, Erlangen Germany) and is equipped with a novel gradient system that is capable of a maximum strength of 300 mT/m (Fan et al., 2014; Setsompop et al., 2013). This is the major hardware component of HCP-driven MR technology innovation. The strong gradient system greatly shortens the time spent on diffusion encoding and decreases signal loss due to T2 decay. We have collected one dataset of 35 healthy adults and are in the process of acquiring a second dataset to include 120 healthy participants spanning a wide age range (8 to 90 years old).

The first dataset, referred to as the *MGH–USC Adult Diffusion Dataset*, demonstrates the capability of the innovative CONNECTOM gradient system for *in vivo* human diffusion MRI (dMRI). In each of the 35 participants, dMRI data with a broad range of *b*-values (1000, 3000, 5000 and 10,000 s/mm²) were collected. The data were minimally preprocessed, and are publically available through open access data repositories. It is

Age Distribution

Fig. 1. Age distribution of the participants of the MGH–USC Adult Diffusion Dataset (N = 35).

Table 2
Imaging parameters of diffusion scans of the MGH–USC Adult Diffusion Dataset.

Parameter	Value
Sequence	Spin-echo EPI
TR/TE (ms)	8800/57
δ/Δ (ms)	12.9/21.8
FOV (mm)	210×210
Acquisition matrix	140×140
Slices	96 axial slices, 1.5 mm thick, 1.5 mm isotropic voxels
iPAT	3
Multiband/SMS factor	1
Echo spacing (ms)	0.63
BW	1984 Hz/Pix
Phase partial Fourier	6/8
b-values	1000, 3000, 5000, 10,000 s/mm^2
Total acquisition time	89 min

SMS = simultaneous multi-slice.

a unique, openly available source of high angular and high spatial resolution dMRI data with high diffusion weighting. One purpose of acquiring and sharing the data is to facilitate studies of new advanced diffusion analysis methods that may rely on contrasts from ultra-high diffusion weighting (i.e. high b-values) to resolve fine details of white matter microstructure perhaps not appreciable with standard gradient MR systems. For this purpose, the data acquisition scheme of the MGH–USC Adult Diffusion Dataset was not tailored specifically for any particular analysis method; rather, it was designed with the intent to allow for as much flexibility for future analyses as possible.

Collection of a second sample with ultra-high diffusion weighting MRI data, referred to as the *MGH–Harvard–USC Lifespan Dataset*, is currently underway and will be shared in the near future. For this second dataset a total of 120 healthy participants ranging from 8 to 90 years old will be scanned to demonstrate the feasibility of ultra-high b-value dMRI across a wide age range and to prepare a reference sample for future studies in patient populations that include children, adolescents, and older adults. In addition to exploring an age range that includes differences in brain development and atrophy, the groups included also vary in their tendency to move during the acquisition, allowing methodological and feasibility explorations of motion effects on measures of white matter microstructure that may be common in studies comparing age groups and patient groups.

All data from the MGH–USC HCP described in this report are publically available through the Laboratory of Neuro Imaging Image Data Archive (LONI IDA) and the WU–Minn Connectome Database (ConnectomeDB). The LONI IDA (https://ida.loni.usc.edu) is an integrated environment for safely archiving, querying and visualizing imaging data utilizing a web-browser interface. Specifically, the LONI IDA is a large-scale archive for neuroimaging, genetics, and phenomic datasets which serves a variety of multi-site imaging programs including the Alzheimer's Disease Neuroimaging Initiative (Toga et al., 2010) and the Michael J. Fox Foundation sponsored Parkinson's Progressive Markers Initiative (http://www.ppmi-info.org), and other major neuroimaging programs. All of the data from the MGH–USC HCP CONNECTOM scanner, described below, are freely available for access, download, or direct workflow submission using LONI Pipeline (Dinov et al., 2010) by any user after a permission request procedure (http://www.humanconnectomeproject.org/data). The WU–Minn HCP consortium maintains the ConnectomeDB (https://db.humanconnectome.org)

to exclusively manage HCP data (Marcus et al., 2013) (see Hodge et al., 2015 for more detailed information about the ConnectomeDB in the same issue).

The MGH–USC Adult Diffusion Dataset ($N = 35$) collection is complete and minimally preprocessed. Both the unprocessed and minimally preprocessed data are available for download through LONI-IDA and ConnectomeDB. Acquisition of the MGH–Harvard–USC Lifespan Dataset is currently underway and, upon the completion of data collection, data processing and quality assessment, unprocessed and minimally preprocessed data will be added to both the LONI IDA and ConnectomeDB repositories for public access. The purpose of the present article is to describe the MGH–USC Adult Diffusion Dataset in detail and to give a flavor of what is to come in terms of the MGH–Harvard–USC Lifespan Dataset.

MGH–USC Adult Diffusion Dataset ($N = 35$)

Participants

All participants provided in the MGH–USC Adult Diffusion Dataset were scanned on the 3T CONNECTOM MRI scanner (see (Setsompop et al., 2013) for an overview) housed at the Athinoula A. Martinos Center for Biomedical Imaging at MGH. A custom-made 64-channel phased array head coil was used for signal reception (Keil et al., 2013). No data were collected on other imaging modalities.

Thirty-five healthy adults participated in this study (16 Females, 20–59 years old; mean age = 31.1 years old). All participants gave written informed consent, and the experiments were carried out with approval from the institutional review board of Partners Healthcare. Participants' gender and age are available in the data sharing repository. No other non-imaging data were collected. Due to the limited sample size there are some ages for which we had only one participant. Given de-identification considerations, age information is provided in 5-year age bins (Fig. 1).

MRI data acquisition

T1w, T2w and diffusion weighted (DW) MRI data were acquired. The T1w images were acquired with a Multi-echo Magnetization-

Table 1
Imaging parameters of structural scans of the MGH–USC Adult Diffusion Dataset.

Type	Description	TR/TE (ms)	TI (ms)	Flip Angle	FOV (mm)	Voxel Size	Band width (Hz/Pix)	iPAT	Acquisition time (min:s)
T1w	3D MPRAGE	2530/1.15	1100	7.0º	256×256	1 mm isotropic	651	2	6:02
T2w	3D T2-SPACE	3200/561	--	--	224×224	0.7 mm isotropic	744	2	6:48

TR/TE = repetition time/echo time; TI = inversion time; FOV = field of view; iPAT = integrated parallel acquisition techniques (GRAPPA acceleration factor).

Table 3
Other details of diffusion scans of the MGH–USC Adult Diffusion Dataset.

Run number	b-value (s/mm²)	Diffusion directions	Acquisition time (min:s)
1	1000	64	11:44
2	3000	64	11:44
3	5000	128 set1	21:51
4	10,000	128 set1	21:51
5	10,000	128 set2	21:51

Prepared Rapid Acquisition Gradient Echo (MEMPRAGE) sequence at 1 mm isotropic resolution (van der Kouwe et al., 2008). T2w data were acquired with a T2-SPACE sequence at 0.7 mm isotropic resolution (Lichy et al., 2005). dMRI data were acquired using a mono-polar Stejskal–Tanner pulsed gradient spin-echo echo planar imaging (EPI) sequence with parallel imaging using Generalized Autocalibrating Partially Parallel Acquisition (GRAPPA). The Fast Low-angle Excitation Echo-planar Technique (FLEET) (Polimeni et al., 2015) was used for Auto-Calibration Signal (ACS) acquisitions to reduce the motion sensitivity of the training data and improve the stability and SNR of the GRAPPA reconstructions. The Simultaneous Multi-Slice (SMS; multi-band) technique (Feinberg et al., 2010; Feinberg and Setsompop, 2013; Setsompop et al., 2012a,b) has been shown to increase the time efficiency of diffusion imaging and was considered for this protocol, however at the point in the project timeline when data acquisition was to begin, the SMS method was not implemented in the EPI sequence featuring FLEET-ACS for GRAPPA. Because of the key benefits of in-plane acceleration for improved EPI data quality, such as lower effective echo spacing and hence mitigated EPI distortions and blurring, and also because of the longer image reconstruction times associated with SMS-EPI data, here data acquisition was performed without the use of SMS in favor of in-plane acceleration using FLEET-ACS and GRAP-PA. (Acquisition of subsequent datasets including the Life Span dataset utilized a more newly implemented sequence combining SMS-EPI with FLEET-ACS and GRAPPA, see below.)

In each subject, dMRI data were collected with 4 different b-values (i.e., 4 shells): 1000 s/mm² (64 directions), 3000 s/mm² (64 directions), 5000 s/mm² (128 directions), and 10,000 s/mm² (256 directions). Different b-values were achieved by varying the diffusion gradient amplitudes, while the gradient pulse duration (δ) and diffusion time (Δ) were held constant. These b-values were chosen to provide some overlap with the HCP data from WU–Minn consortium, while at the same time push to the limit of diffusion weighting within the constraints of SNR and acquisition time. On determining the number of directions in
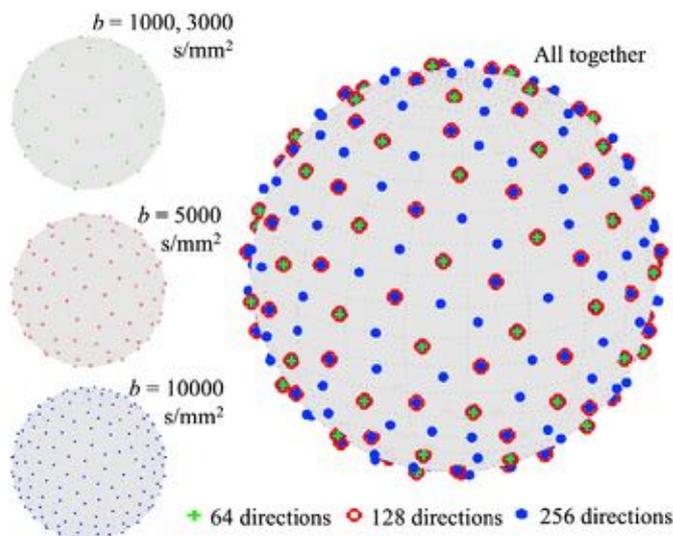
each shell, in general, data with higher b-value were acquired with more DW directions to capture the increased ratio of high angular frequency components in the MR signal, and to compensate for the SNR loss due to increased diffusion weighting. Also, the number of directions in each shell was selected to meet the typical requirements of popular single shell and multi-shell analysis methods (e.g. q-ball imaging (Descoteaux et al., 2007; Tuch, 2004; Tuch et al., 2002; Tuch et al., 2003), spherical deconvolution (Anderson, 2005; Dell'Acqua et al., 2007; Tournier et al., 2004), ball and stick model (Behrens et al., 2007; Jbabdi et al., 2012), multi-shell q-ball imaging (Aganj et al., 2010; Yeh et al., 2010), diffusion propagator imaging (Descoteaux et al., 2009, 2011), etc.), and to keep the total acquisition time feasible in healthy control subjects.

The diffusion sensitizing direction sets were specifically designed so that the 64-direction set is a subset of the 128-direction set, which is again a subset of the 256-direction set (Fig. 2). The initial 64 directions were calculated with the electro-static repulsion method (Caruyer et al., 2013; Jones et al., 1999). With these 64 directions fixed, another 64 directions were added as unknowns, and an optimized 128-direction set was calculated by adjusting the added 64 directions using electro-static repulsion optimization. With these 128 directions fixed, the 256-direction set was generated using the same method. As such, all 4 shells share the same 64 directions; the $b = 5000$ s/mm² shell and the $b = 10,000$ s/mm² shell share the same 128 directions.

During data acquisition, the diffusion sensitizing directions with approximately opposite polarities were played in pairs to counter-balance the eddy current effects induced by switching the diffusion weighting gradient on and off. Each run started with acquiring a non-DW image ($b = 0$), and one non-DW image was collected every 13 DW images thereafter. Therefore 552 image volumes were collected in total, including 512 DW and 40 non-DW volumes for each subject. More detailed imaging parameters are listed in Tables 1, 2, and 3. Full imaging protocols can be found in both data repositories.

In summary, the imaging protocol was tailored to be suitable for a variety of both single and multi-shell reconstruction methods, so that off-site researchers with their own analysis methods yet no direct access to a dedicated CONNECTOM scanner can benefit from the data release.

MRI data preprocessing and quality control

All MRI data were corrected for gradient nonlinearity distortions offline (Glasser et al., 2013; Jovicich et al., 2006). Diffusion data were further corrected for head motion and eddy current artifacts. Specifically, the $b = 0$ images interspersed throughout the diffusion scans were used to estimate bulk head movements with respect to the initial time point (the first $b = 0$ image), where rigid transformation was calculated using the boundary based registration tool in the FreeSurfer package V5.3.0 (Greve and Fischl, 2009). For each $b = 0$ image, this transformation was then applied to itself and to the following 13 diffusion weight-ed images to correct for head motion. Data of all 4 b-values were concatenated (552 image volumes in total) and passed into the EDDY tool (Andersson et al., 2012) for eddy current distortion correction and residual head motion estimates. The rigid rotational components of the motion estimates were then used to adjust the diffusion gradient table for later data reconstruction purposes. To de-identify the high

Fig. 2. Gradient direction sets of the MGH–USC Adult Diffusion Dataset.

Table 4
Age distribution of participants of the MGH–Harvard–USC Lifespan Dataset.

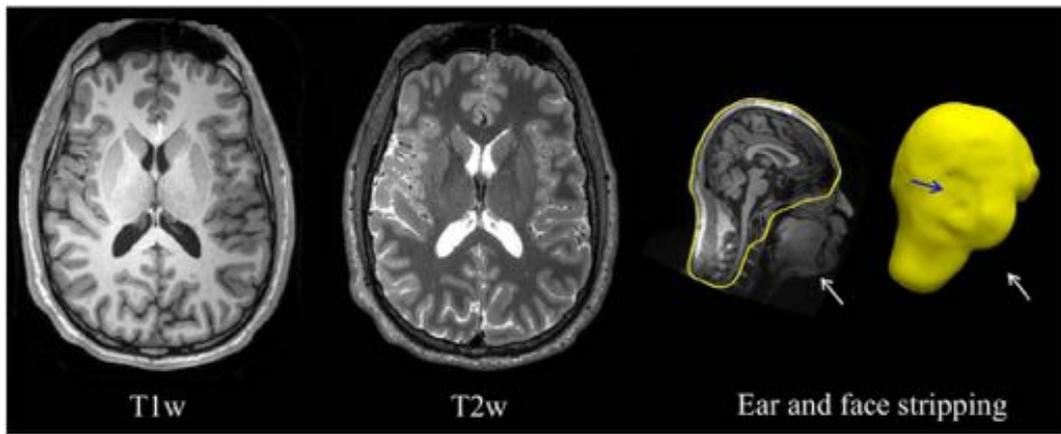| Cohort	Age range (years old)	Target sample size
Children	8–11	20
	12–14	20
	15–17	20
Young adults	18–28	20
Older adults	50–65	20
	66–90	20

Fig. 3. Anatomical scans. An axial plane of the T1w, T2w scans, and the mask used for ear (blue arrow) and face (white arrows) stripping are shown.

resolution T1w and T2w anatomical scans, face and ear regions were masked while the skull was retained as much as possible to accommodate future skull stripping and brain parcellation efforts. Users of the data should be aware that skull stripping can have subtle effects of data processing and morphometric quantification (Holmes et al., 2015).

Both unprocessed and minimally preprocessed data are available for download in compressed NIfTI format. The measured gradient field nonlinearity coefficients are protected by Siemens as proprietary information. Because the gradient nonlinearity correction cannot be performed without this information, the unprocessed data provided have already been corrected for gradient nonlinearity distortions with no other preprocessing performed. The unprocessed T1w and T2w additionally have face and ear regions stripped.

All the anatomical scans (T1w and T2w) were free from gross brain abnormalities as determined by a trained physician. All MRI data (T1w, T2w and DW) went through the process of quality assessment by a faculty member, a postdoctoral researcher and a research assistant, all trained in neuroimaging. More specifically, each dataset was assessed by two raters, who viewed both the unprocessed and minimally preprocessed data volume by volume, and rated in terms of head movements, facial and ear mask coverage (to make sure that brain tissue was not masked off), and eddy current correction results. Finally, a comprehensive grade was given to determine whether a dataset had passed quality control.

To cite the MGH Adult Diffusion Dataset, use the LONI IDA URL: http://www.humanconnectomeproject.org (see also http://www.humanconnectomeproject.org/data for more instructions on acknowledging the use of data), or use the WU–Minn ConnectomeDB URL https://db.humanconnectome.org/data/projects/MGH_DIFF.

MGH–Harvard–USC Lifespan Dataset (target $N = 120$)

Data collection for the MGH–Harvard–USC Lifespan Dataset is underway. T1w, T2w, resting-state fMRI, and dMRI data of 120 healthy study participants ranging from children to older adults will be shared. The specific age ranges for each group and target sample sizes are listed in Table 4. Extensive cognitive or neuropsychological data will not be available for this feasibility study; however, basic demographic variables will be publically available, including age, gender, years of education, social economic status, and an estimate of IQ. The MGH–Harvard–USC Lifespan protocol is based on the healthy adult study, but slightly modified to accommodate lower tolerance for long scanning sessions in the children and older adults. T1w and T2w anatomical images are acquired with an MEMPRAGE and T2-SPACE sequence respectively, both at 1 mm isotropic resolution, and both with acquisition times under 4 min.

Diffusion data are acquired using a spin echo EPI sequence with a GRAPPA factor of 3 combined with FLEET-ACS acquisition. A SMS factor of 2 is used allowing for faster data acquisition. Diffusion data acquisition is performed at two different b-values: 2500 s/mm^2 (60 DW directions) and 7500 s/mm^2 (180 DW directions). Resting state BOLD fMRI data are acquired for the MGH–Harvard–USC Lifespan Dataset and will be shared. One or two runs of 6 min 6 s each will be acquired in each participant. Data preprocessing and quality control procedures
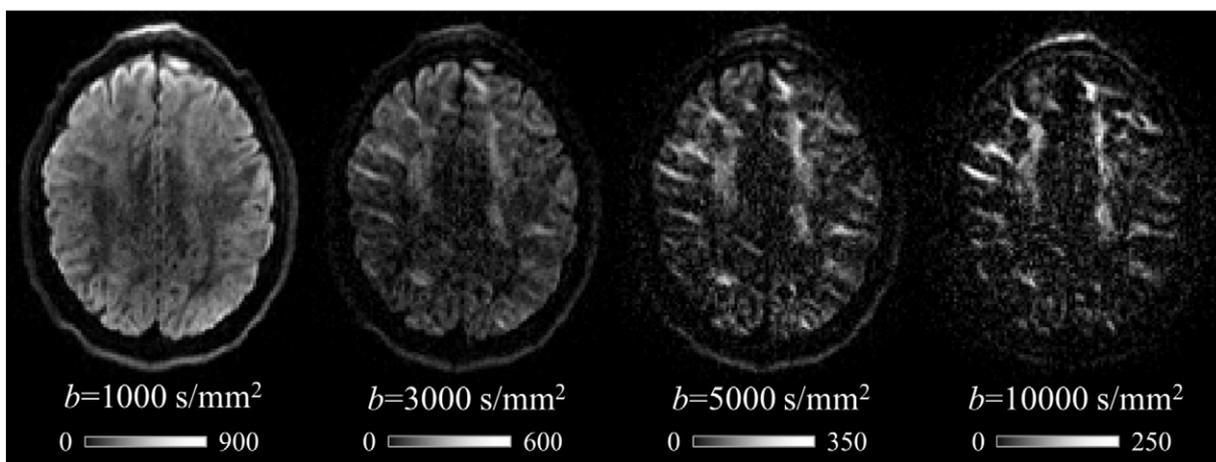

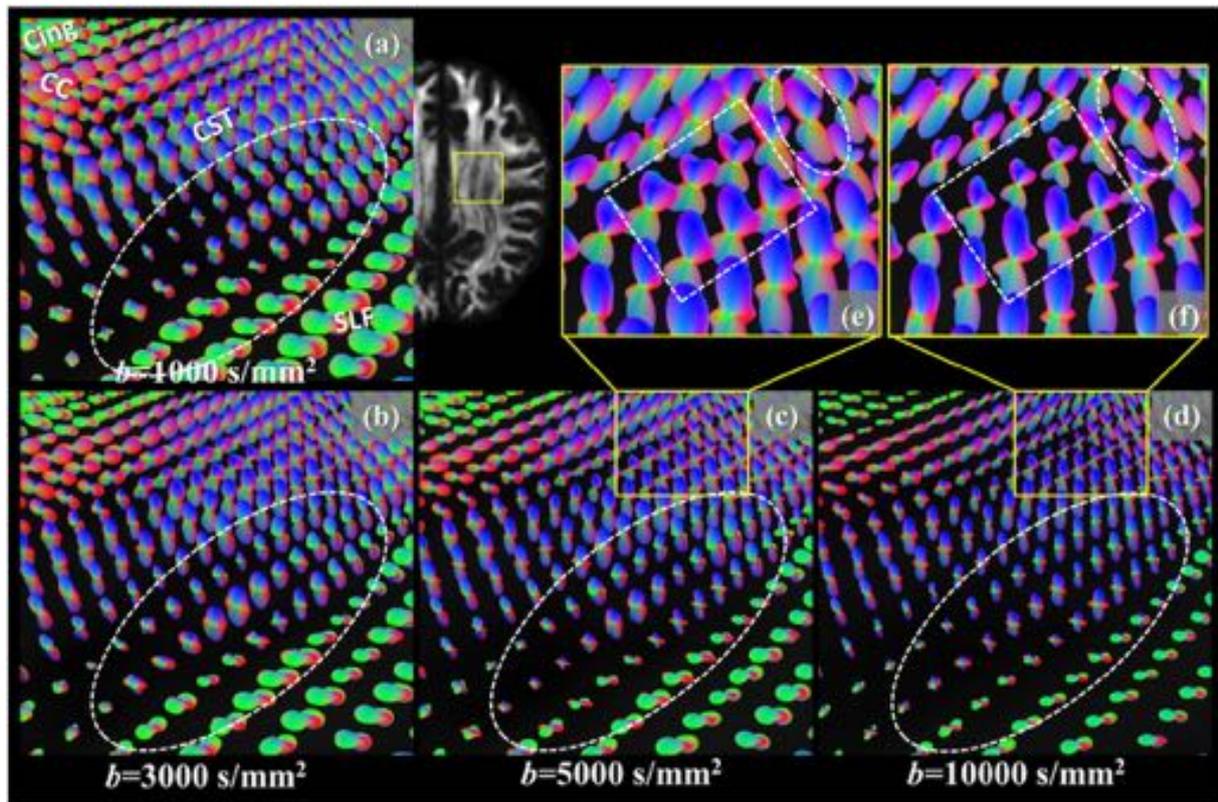**Fig. 4.** DW images at different b-values. Intensity scales were adjusted to better reveal the image contrasts.

Fig. 5. *q*-ball ODF reconstruction of dMRI data with (a) *b* = 1000 s/mm², (b) *b* = 3000 s/mm², (c) *b* = 5000 s/mm², and (d) *b* = 10,000 s/mm² in the centrum semiovale. For *b* = 5000 and 10,000 s/mm², the region circled in yellow (c–d) was zoomed-in and shown in (e–f). The territories of major fiber tracts were labeled in (a): Cing = cingulate; CC = corpus callosum; CST = corticospinal tract; SLF = superior longitudinal fasciculus.

will be comparable to the methods used for MGH–USC Adult Diffusion Dataset.

Data access

The MGH–USC Adult Diffusion Dataset is openly available. Users must register with either LONI IDA (https://ida.loni.usc.edu/services/NewUser.jsp) or ConnectomeDB (https://db.humanconnectome.org/app/template/Login.vm) to get access to the data. All imaging and demographic data are directly available for download from either of the two repositories. Data Usage Agreements are required (for more details on the Data Usage Agreement with LONI IDA, see https://ida.

loni.usc.edu/collaboration/access/appLicense.jsp; for more details of Data Use Terms with ConnectomeDB, see http://humanconnectome.org/data/data-use-terms/index.html).

For updates, at LONI IDA, as new datasets are added to the HCP collection, registered users are notified via email so that they may examine and explore these additional data. At ConnectomeDB, updates on data withdrawal/revision/addition are posted on the HCP Data Releases page (http://humanconnectome.org/data/).

Regarding the handling of large dataset requests, users may search the LONI IDA HCP archive for specific datasets or may download the complete set of images at once. Downloads are governed by dedicated compute servers which balance and schedule loads appropriately across
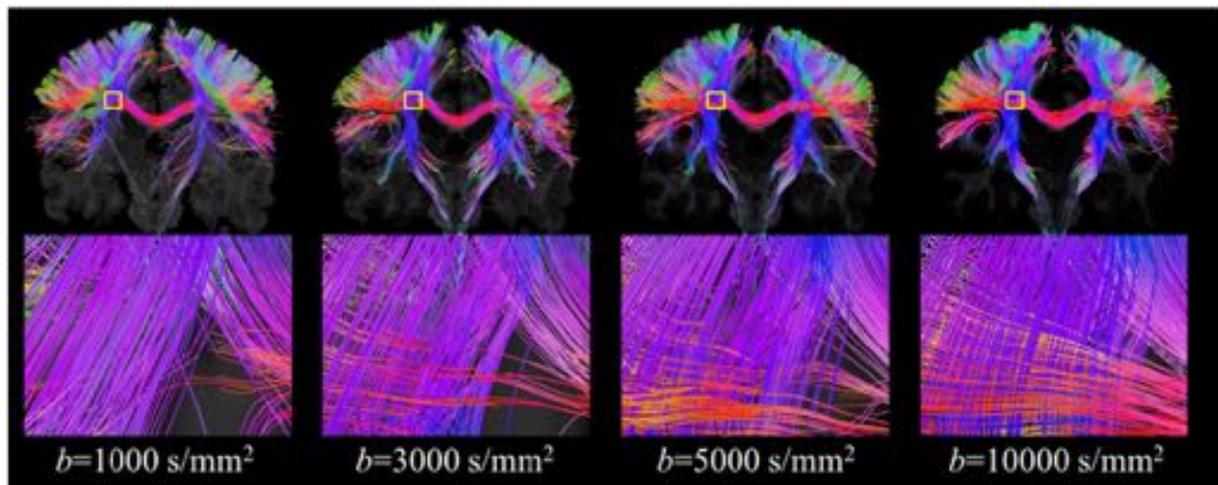

Fig. 6. Front view of the fiber tracts reconstructed from dMRI data with different *b*-values. Streamlines passing by either of the bi-lateral postcentral gyri were selected and shown. For different *b*-values, the same region in the centrum semiovale was circled in yellow and zoomed-in to reveal the difference.
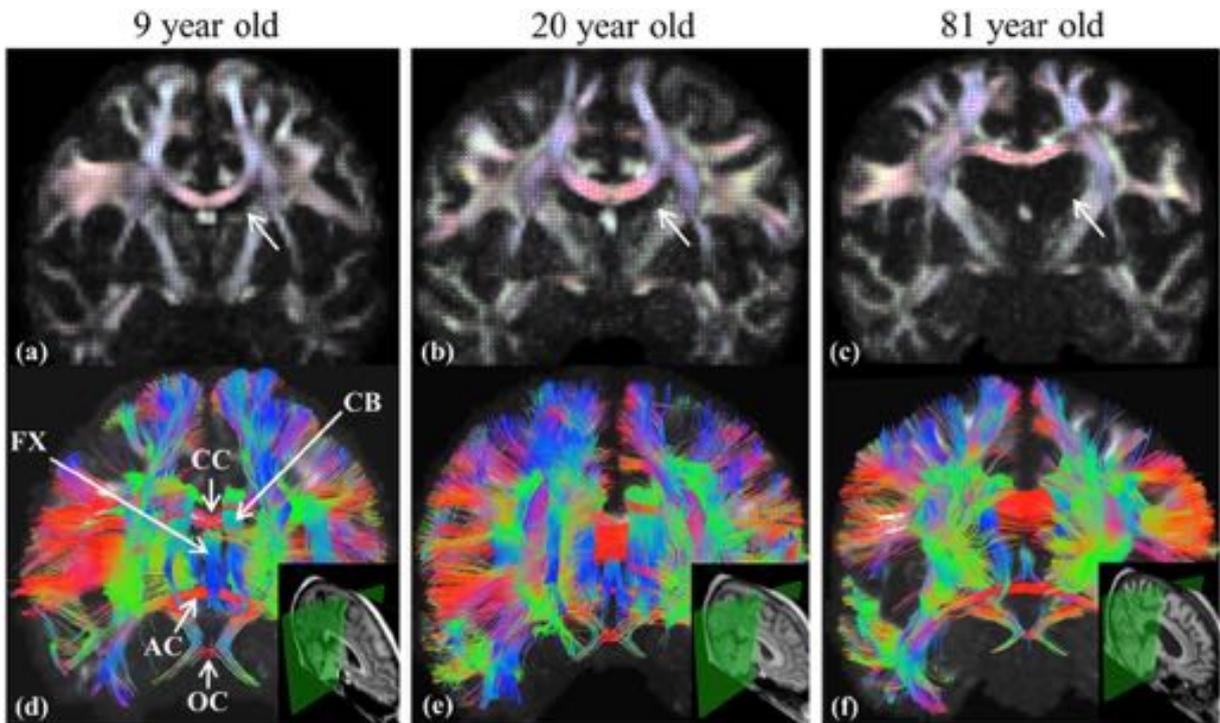
Fig. 7. Feasibility of high *b*-value dMRI across the lifespan. GQI ODF reconstruction of multi-shell dMRI data in three example subjects from different age cohorts (a–c). Enlarged ventricles in the older adult indicate age-associated brain atrophy (c). Tractography results show major and fine inter-hemispheric white matter bundles in all three cases. Tracts are labeled in (d): FX = fornix; CC = corpus callosum; CB = cingulate bundle; AC = anterior commissure; OC = optic chiasm.

multiple CPUs to maintain high levels of data delivery performance. At ConnectomeDB, a commercial UDP-based data transfer technology called Aspera fasp™ (http://asperasoft.com) is used to support high speed downloads. A downloadable plug-in, available free of charge, is required to enable Aspera-based transfers (see also Hodge et al., 2015).

The MGH–USC Adult Diffusion Dataset is managed and maintained on the LONI IDA for long term accessibility. All CONNECTOM users are encouraged to archive and share their data on the LONI IDA platform. To archive the data, it is required to go through an online automatic pipeline of de-identification and relevant metadata extraction.

Demonstration of MGH–USC HCP datasets

MGH–USC Adult Diffusion Datasets

Here we briefly illustrate the data type and quality of the MGH–USC Adult Diffusion Datasets, using one example dataset.

Fig. 3 shows an axial plane of the T1w and T2w scans, along with the mask used for ear and face stripping. Data shown were corrected for gradient nonlinearity distortions.

Fig. 4 shows an axial plane of the preprocessed dMRI data with diffusion weighting applied along the same direction but with different gradient strengths.

Fig. 5 shows the *q*-ball Orientation Distribution Function (ODF) reconstruction obtained from the dMRI data with different *b*-values. DSI-Studio (http://dsi-studio.labsolver.org) was used to calculate and visualize ODFs. The ODFs were calculated with a maximum spherical harmonic order of 8, and a *Laplace–Beltrami* regularization weight parameter of $\lambda = 0.006$ (Descoteaux et al., 2007).

Fig. 6 shows the fiber tracking results obtained from the dMRI data with different *b*-values. DSI-Studio was used to calculate and visualize the fiber tracts. Tractography was performed with default parameters. Fiber tracts passing through either of the bi-lateral postcentral gyri were selected and shown, where the masks for the postcentral gyri were obtained from the standard FreeSurfer parcellation.

MGH–Harvard–USC Lifespan Datasets

Fig. 7 demonstrates feasibility of high *b*-value dMRI across the lifespan. The dMRI data of $b = 2500$ and 7500 s/mm² were combined and analyzed using the generalized *q*-sampling imaging (GQI) reconstruction in DSI Studio (Yeh et al., 2010), which was then used for diffusion tractography. Results are displayed in each individual's native space. As shown, some age-associated morphometric changes are evident, such as brain atrophy in the older adult as indicated by the enlarged ventricles (Fig. 7 a–c). Tractography results show major and fine inter-hemispheric white matter bundles such as the corpus callosum and the anterior commissure. One can also recognize the fornix in each of the three participants, as well as contours of the optic chiasm (Fig. 7 d–f).

Conclusion

Based on the 3T Siemens CONNECTOM system, the MGH–USC HCP datasets serve as a unique openly available source of high angular and spatial resolution dMRI data with *b*-values up to 10,000 s/mm². The ongoing MGH–Harvard–USC Lifespan study will further add to the database by providing data across the age span from children to older adults.

Acknowledgments

References

Aganj, I., Lenglet, C., Sapiro, G., Yacoub, E., Ugurbil, K., Harel, N., 2010. Reconstruction of the orientation distribution function in single- and multiple-shell q-ball imaging within constant solid angle. Magn. Reson. Med. 64, 554–566.

Anderson, A.W., 2005. Measurement of fiber orientation distributions using high angular resolution diffusion imaging. Magn. Reson. Med. 54, 1194–1206.

Andersson, J.L., Xu, J., Yacoub, E., Auerbach, E., Moeller, S., Ugurbil, K., 2012. A comprehensive Gaussian process framework for correcting distortions and movements in diffusion images. Proc. Int. Soc. Magn. Reson. Med. 2426.

Behrens, T.E., Berg, H.J., Jbabdi, S., Rushworth, M.F., Woolrich, M.W., 2007. Probabilistic diffusion tractography with multiple fibre orientations: what can we gain? NeuroImage 34, 144–155.

Caruyer, E., Lenglet, C., Sapiro, G., Deriche, R., 2013. Design of multishell sampling schemes with uniform coverage in diffusion MRI. Magn. Reson. Med. 69, 1534–1540.

Dell'Acqua, F., Rizzo, G., Scifo, P., Clarke, R.A., Scotti, G., Fazio, F., 2007. A model-based deconvolution approach to solve fiber crossing in diffusion-weighted MR imaging. IEEE Trans. Biomed. Eng. 54, 462–472.

Descoteaux, M., Angelino, E., Fitzgibbons, S., Deriche, R., 2007. Regularized, fast, and robust analytical Q-ball imaging. Magn. Reson. Med. 58, 497–510.

Descoteaux, M., Deriche, R., Le Bihan, D., Mangin, J.F., Poupon, C., 2009. Diffusion propagator imaging: using Laplace's equation and multiple shell acquisitions to reconstruct the diffusion propagator. Inf Process Med Imaging 21, 1–13.

Descoteaux, M., Deriche, R., Le Bihan, D., Mangin, J.F., Poupon, C., 2011. Multiple q-shell diffusion propagator imaging. Med. Image Anal. 15, 603–621.

Dinov, I., Lozev, K., Petrosyan, P., Liu, Z., Eggert, P., Pierce, J., Zamanyan, A., Chakrapani, S., Van Horn, J., Parker, D.S., Magsipoc, R., Leung, K., Gutman, B., Woods, R., Toga, A., 2010. Neuroimaging study designs, computational analyses and data provenance using the LONI pipeline. PLoS ONE 5.

Fan, Q., Nummenmaa, A., Witzel, T., Zanzonico, R., Keil, B., Cauley, S., Polimeni, J.R., Tisdall, D., Van Dijk, K.R., Buckner, R.L., Wedeen, V.J., Rosen, B.R., Wald, L.L., 2014. Investigating the capability to resolve complex white matter structures with high b-value diffusion magnetic resonance imaging on the MGH–USC Connectom scanner. Brain Connect. 4, 718–726.

Feinberg, D.A., Setsompop, K., 2013. Ultra-fast MRI of the human brain with simultaneous multi-slice imaging. J. Magn. Reson. 229, 90–100.

Feinberg, D.A., Moeller, S., Smith, S.M., Auerbach, E., Ramanna, S., Gunther, M., Glasser, M.F., Miller, K.L., Ugurbil, K., Yacoub, E., 2010. Multiplexed echo planar imaging for sub-second whole brain FMRI and fast diffusion imaging. PLoS ONE 5, e15710.

Glasser, M.F., Sotiropoulos, S.N., Wilson, J.A., Coalson, T.S., Fischl, B., Andersson, J.L., Xu, J., Jbabdi, S., Webster, M., Polimeni, J.R., Van Essen, D.C., Jenkinson, M., Consortium, W.-M.H., 2013. The minimal preprocessing pipelines for the Human Connectome Project. NeuroImage 80, 105–124.

Greve, D.N., Fischl, B., 2009. Accurate and robust brain image alignment using boundary-based registration. NeuroImage 48, 63–72.

Hodge, M.R., Horton, W., Brown, T., Herrick, R., Olsen, T., Hileman, M.E., McKay, M., Archie, K.A., Cler, E., Harms, M.P., Burgess, G.C., Glasser, M.F., Elam, J.S., Curtiss, S.W., Barch, D.M., Oostenveld, R., Larson-Prior, L.J., Ugurbil, K., Van Essen, D.C., Marcus, D.S., 2015. ConnectomeDB—Sharing human brain connectivity data. NeuroImage. http://dx.doi.org/10.1016/j.neuroimage.2015.04.046.

Holmes, A., Hollinshead, M., O'Keefe, T., Petrov, V., Fariello, G., Wald, L., Fischl, B., Rosen, B., Mair, R., Roffman, J., Smoller, J., Buckner, R., 2015w. The Brain Genomics Superstruct Project (GSP) initial data release: structural, functional, and behavioral measures. Nat Sci Data 2, 150031.

Jbabdi, S., Sotiropoulos, S.N., Savio, A.M., Graña, M., Behrens, T.E., 2012. Model-based analysis of multishell diffusion MR data for tractography: how to get over fitting problems. Magn. Reson. Med. 68, 1846–1855.

Jones, D.K., Horsfield, M.A., Simmons, A., 1999. Optimal strategies for measuring diffusion in anisotropic systems by magnetic resonance imaging. Magn. Reson. Med. 42, 515–525.

Jovicich, J., Czanner, S., Greve, D., Haley, E., van der Kouwe, A., Gollub, R., Kennedy, D., Schmitt, F., Brown, G., Macfall, J., Fischl, B., Dale, A., 2006. Reliability in multi-site structural MRI studies: effects of gradient non-linearity correction on phantom and human data. NeuroImage 30, 436–443.

Keil, B., Blau, J.N., Biber, S., Hoecht, P., Tountcheva, V., Setsompop, K., Triantafyllou, C., Wald, L.L., 2013. A 64-channel 3T array coil for accelerated brain MRI. Magn. Reson. Med. 70, 248–258.

Lichy, M.P., Wietek, B.M., Mugler, J.P., Horger, W., Menzel, M.I., Anastasiadis, A., Siegmann, K., Niemeyer, T., Königsrainer, A., Kiefer, B., Schick, F., Claussen, C.D., Schlemmer, H.P., 2005. Magnetic resonance imaging of the body trunk using a single-slab, 3-dimensional, T2-weighted turbo-spin-echo sequence with high sampling efficiency (SPACE) for high spatial resolution imaging: initial clinical experiences. Investig. Radiol. 40, 754–760.

Marcus, D.S., Harms, M.P., Snyder, A.Z., Jenkinson, M., Wilson, J.A., Glasser, M.F., Barch, D.M., Archie, K.A., Burgess, G.C., Ramaratnam, M., Hodge, M., Horton, W., Herrick, R., Olsen, T., McKay, M., House, M., Hileman, M., Reid, E., Harwell, J., Coalson, T., Schindler, J., Elam, J.S., Curtiss, S.W., Van Essen, D.C., Consortium, W.-M.H., 2013. Human Connectome Project informatics: quality control, database services, and data visualization. NeuroImage 80, 202–219.

Polimeni, J., Bhat, H., Witzel, T., Benner, T., Feiweier, T., Inati, S., Renvall, V., Heberlein, K., Wald, L., 2015. Reducing sensitivity losses due to respiration and motion in accelerated echo planar imaging by reordering the auto-calibration data acquisition. Magn. Reson. Med. http://www.ncbi.nlm.nih.gov/pubmed/25809559.

Setsompop, K., Cohen-Adad, J., Gagoski, B.A., Raij, T., Yendiki, A., Keil, B., Wedeen, V.J., Wald, L.L., 2012a. Improving diffusion MRI using simultaneous multi-slice echo planar imaging. NeuroImage 63, 569–580.

Setsompop, K., Gagoski, B.A., Polimeni, J.R., Witzel, T., Wedeen, V.J., Wald, L.L., 2012b. Blipped-controlled aliasing in parallel imaging for simultaneous multislice echo planar imaging with reduced g-factor penalty. Magn. Reson. Med. 67, 1210–1224.

Setsompop, K., Kimmlingen, R., Eberlein, E., Witzel, T., Cohen-Adad, J., McNab, J.A., Keil, B., Tisdall, M.D., Hoecht, P., Dietz, P., Cauley, S.F., Tountcheva, V., Matschl, V., Lenz, V.H., Heberlein, K., Potthast, A., Thein, H., Van Horn, J., Toga, A., Schmitt, F., Lehne, D., Rosen, B.R., Wedeen, V., Wald, L.L., 2013. Pushing the limits of in vivo diffusion MRI for the Human Connectome Project. NeuroImage 80, 220–233.

Toga, A.W., Crawford, K.L., Alzheimer's Disease Neuroimaging, I., 2010. The informatics core of the Alzheimer's Disease Neuroimaging Initiative. Alzheimers Dement. 6, 247–256.

Tournier, J.D., Calamante, F., Gadian, D.G., Connelly, A., 2004. Direct estimation of the fiber orientation density function from diffusion-weighted MRI data using spherical deconvolution. NeuroImage 23, 1176–1185.

Tuch, D.S., 2004. Q-ball imaging. Magn. Reson. Med. 52, 1358–1372.

Tuch, D.S., Reese, T.G., Wiegell, M.R., Makris, N., Belliveau, J.W., Wedeen, V.J., 2002. High angular resolution diffusion imaging reveals intravoxel white matter fiber heterogeneity. Magn. Reson. Med. 48, 577–582.

Tuch, D.S., Reese, T.G., Wiegell, M.R., Wedeen, V.J., 2003. Diffusion MRI of complex neural architecture. Neuron 40, 885–895.

van der Kouwe, A.J., Benner, T., Salat, D.H., Fischl, B., 2008. Brain morphometry with multiecho MPRAGE. NeuroImage 40, 559–569.

Yeh, F.C., Wedeen, V.J., Tseng, W.Y., 2010. Generalized q-sampling imaging. IEEE Trans. Med. Imaging 29, 1626–1635.